

Are we certain it's anomalous?

Alessandro Flaborea , Bardh Prenkaj , Bharti Munjal , Marco Aurelio Sterpa , Dario Aragona , Luca Podo , and Fabio Galasso

Abstract—The progress in modelling time series and, more generally, sequences of structured-data has recently revamped research in anomaly detection. The task stands for identifying abnormal behaviours in financial series, IT systems, aerospace measurements, and the medical domain, where anomaly detection may aid in isolating cases of depression and attend the elderly. Anomaly detection in time series is a complex task since anomalies are rare due to highly non-linear temporal correlations and since the definition of anomalous is sometimes subjective.

Here we propose the novel use of Hyperbolic uncertainty for Anomaly Detection (HypAD). HypAD learns self-supervisedly to reconstruct the input signal. We adopt best practices from the state-of-the-art to encode the sequence by an LSTM, jointly learnt with a decoder to reconstruct the signal, with the aid of GAN critics. Uncertainty is estimated end-to-end by means of a hyperbolic neural network. By using uncertainty, HypAD may assess whether it is certain about the input signal but it fails to reconstruct it because this is anomalous; or whether the reconstruction error does not necessarily imply anomaly, as the model is uncertain, e.g. a complex but regular input signal. The novel key idea is that a *detectable anomaly* is one where the model is certain but it predicts wrongly.

HypAD outperforms the current state-of-the-art for univariate anomaly detection on established benchmarks based on data from NASA, Yahoo, Numenta, Amazon, Twitter. It also yields state-of-the-art performance on a multivariate dataset of anomaly activities in elderly home residences, and it outperforms the baseline on SWaT. Overall, HypAD yields the lowest false alarms at the best performance rate, thanks to successfully identifying detectable anomalies.

Index Terms—Anomaly Detection, Time Series, Hyperbolic Neural Networks, Uncertainty Estimation

I. INTRODUCTION

Anomaly detection stands for detecting outliers (anomalies) in data, i.e. points that deviate significantly from the distribution of the data. Outlier detection, however, is an under-specified and consequently ill-posed task due to its inherent unsupervised nature. Anomaly detection strategies such as distance-based [1], [2], density-based [3], [4], and subspace-based methods [5], [6] have been pioneers in the literature. Additionally, autoencoders [7], [8], and adversarial networks [9]

This document is a result of the research project funded by MIUR under the grant of “Dipartimenti di eccellenza 2018-2022” of the Department of Computer Science of Sapienza University of Rome.

Alessandro Flaborea, Bardh Prenkaj, Marco Aurelio Sterpa, Dario Aragona, Luca Podo, and Fabio Galasso are with the Computer Science Dpt. of Sapienza University of Rome, Via Salaria 113, Rome, Italy (emails: [flaborea,prekaj,aragona,podo,galasso]@di.uniroma1.it).

Bharti Munjal is with the OSRAM Research Group and the Technical University of Munich, Parkring 33, 85748 Garching b. Munich (email: m.bharti@osram.com).

© 2022 IEEE. Personal use of this material is permitted. Permission from IEEE must be obtained for all other uses, in any current or future media, including reprinting/republishing this material for advertising or promotional purposes, creating new collective works, for resale or redistribution to servers or lists, or reuse of any copyrighted component of this work in other works.

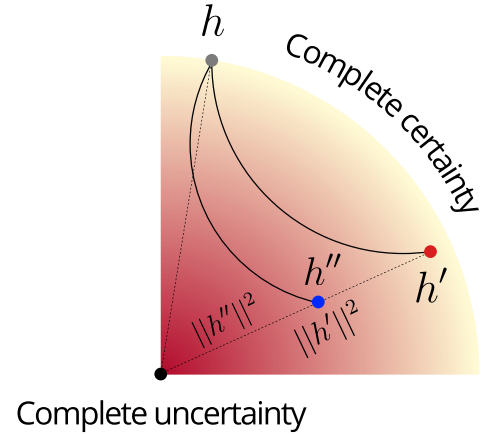


Fig. 1. HypAD detects anomalies by the joint use of reconstruction error and uncertainty, learning both aspects end-to-end. In the illustration, the colored circular sector represents the hyperbolic Poincaré ball, where the radius distance of data embeddings is their degree of certainty (points on the circumference are most certain). h is the hyperbolic mapping of the input signal, which HypAD attempts to match by the reconstruction h' . Thanks to hyperbolic neural networks and their exponentially larger penalization for errors at high certainty, HypAD learns to prefer signal reconstructions such as h'' , i.e. with the same amount of error as h' (the same angle and cosine distance) but smaller radius $\|h''\|^2$ and thus higher uncertainty. HypAD uses both the reconstruction error and the uncertainty to identify detectable anomalies, where the model is certain but the prediction is wrong, i.e. it knows what to expect but something anomalous occurs.

have given a substantial contribution. However, the literature neglects assessing the trustfulness of the predicted outcomes, namely their uncertainty.

Uncertainty is a measure of model confidence, which may be learnt from the data [10], [11] or by the use of extra instances [12]. Uncertainty estimation has been a long-standing challenge in machine learning. Most recently, it has been successfully adopted to improve performance on object detection [13]–[16], pose estimation [17], unsupervised and self-supervised learning [18]–[20]. Yet, uncertainty remains largely unexplored in the context of anomaly detection.

In this work, we propose a novel model based on Hyperbolic uncertainty for Anomaly Detection, which we dub HypAD. We leverage the current state-of-the-art technique for anomaly detection in univariate time series, TadGAN [9]. TadGAN detects anomalies by attempting to reconstruct the input signal, making use of an LSTM sequence encoding and two GAN critics, cf. Sec. III-A. We introduce uncertainty into the anomaly detector: we map the input and the reconstructed signal into a hyperbolic space, where the signals additionally have an uncertainty score; and we train the novel embeddings end-to-end with a Poincaré distance loss, cf. Sec. III-B.

The proposed HypAD uses uncertainty to discern whether the reconstruction error is large because the signal is anomalous, or simply because the model cannot reconstruct it well. In the former case, HypAD is certain about the reconstruction (e.g. most signal is well-behaved and the model expects known patterns) but its reconstruction is wrong, as a part of the signal is anomalous. In the latter, HypAD downgrades its anomaly score because it is not certain about the signal reconstruction. This may be because of a complex pattern, which the model did not have enough capacity to learn. The larger uncertainty indicates that the larger reconstruction error may be due to anomaly or to a model failure in the reconstruction. (See discussion in Sec III-B2.)

Thanks to uncertainty, HypAD outperforms the state-of-the-art univariate anomaly detector TadGAN [9] on the established univariate benchmarks of NASA, Yahoo, Numenta Anomaly Benchmark [21], as well as on two multivariate datasets of daily activities in elderly home residences CASAS [22] and industrial water treatment plant SWaT [23]. As we show in experimental results in Sec. IV, reducing anomaly scores in uncertain cases also yields fewer false alarms (the model achieves best F1 performance with larger precision).

The main contributions of this work are:

- We propose the first model for anomaly detection based on hyperbolic uncertainty;
- We propose the novel key idea of *detectable anomaly*: an instance is anomalous when the model is certain about it but wrong;
- We integrate the estimated uncertainty into a state-of-the-art univariate anomaly detector and consistently outperform it on established univariate and multivariate datasets.

II. RELATED WORKS

To the best of our knowledge, this is the first work to have combined anomaly detection with uncertainty estimation, and the first work to have further proposed hyperbolic uncertainty for it. Previous work relates to ours from three main perspectives, which we review here: uncertainty estimation techniques, anomaly detection in time series and hyperbolic neural networks.

A. Uncertainty Estimation Techniques

We identified two different strategies of approximating uncertainty. *Ensemble-based posterior approximation* uses several weak models to make naive predictions and combine them according to a consensus function into a more complex predictive model [24]. One of the most popular approaches to uncertainty estimation based on ensembles is Monte Carlo (MC) Dropout. It drops neurons on every layer during training and test phases [12].

Generative models for aleatory modelling use an additional latent variable to make stochastic predictions and evaluate the uncertainty of the model. Generative Adversarial Networks (GANs) [25] play a minmax game where the discriminator needs to distinguish between real examples and the generated outcomes. GANs have state-of-the-art performances and we build on top of that by attaching hyperspace mapping layers

to estimate the uncertainty of the model. Another interesting approach to estimate uncertainty is by using energy-based models [26]–[28]. They learn an energy function that models the compatibility of the input and the output. Our method transcends energy-based models because the integrated hyperbolic uncertainty mechanism does not suffer from cold- nor warm-start problems [29] which undermine the training complexity [30].

B. Anomaly Detection in Time Series

We identified five categories of methods proposed in the literature for anomaly detection in time series. *Distance-based* outlier detectors consider the distance of a point from its k -nearest neighbours [2], [31], [32]. *Density-based* methods [3], [4], [33]–[37] take into account the density of the point and its neighbours. *Prediction-based methods* [38]–[40] calculate the difference between the predicted value and the true value to detect anomalies. *Reconstruction based* methods [41]–[43] compare the input signal and the reconstructed one in the output layer typically by using autoencoders. These methods assume that anomalies are difficult to reconstruct and are lost when the signal gets mapped to lower dimensions, thus a higher reconstruction error means higher anomaly score. [42] uses an LSTM autoencoder for multi-sensor anomaly detection. [7], [8] use an ensemble of autoencoders to boost performances by focusing on learning the inlier characteristics at each iteration. [44] uses a hierarchical variational auto-encoder with two stochastic latent variables to learn the temporal and inter-metric embeddings for multivariate data. SISVAE [45] uses a variational auto-encoder with a smoothness-inducing prior over possible estimations to capture latent temporal structures of time series without relying on the assumption of constant noise. Recently, GANs have been employed to detect anomalies in time series data. Our method also lies in this category. MAD-GAN [46] combines the discriminator output and reconstruction error to detect anomalies in multivariate time series. BeatGAN [47] uses encoder-decoder generator with a modified time-warping-based data augmentation to detect anomalies in medical ECG inputs. TadGAN [9] uses a cycle-consistent GAN architecture with an encoder-decoder generator and additionally proposes several ways to compute reconstruction error and its combination with the critic outputs. We build on top of TadGAN's architecture by incorporating the hyperbolic mapping layer to the reconstructed time-windows to assess the uncertainty of the detector.

C. Hyperbolic Neural Networks

Deep representation learning in hyperspaces has gained momentum after the pioneering work of hyperNNs [48] that generalises Euclidean operations (e.g. matrix multiplications) to their counterparts in hyperspace. The authors propose analogue counterparts in hyperspace of neural network components such as fully-connected (FC) layers, multinomial logistic regression (MLR) and recurrent neural networks. Furthermore, methods like Einstein midpoint [49] and Fréchet mean [50] propose different ways of aggregating features in hyperspace. The work in [51] extends hyperNN and proposes Poincaré

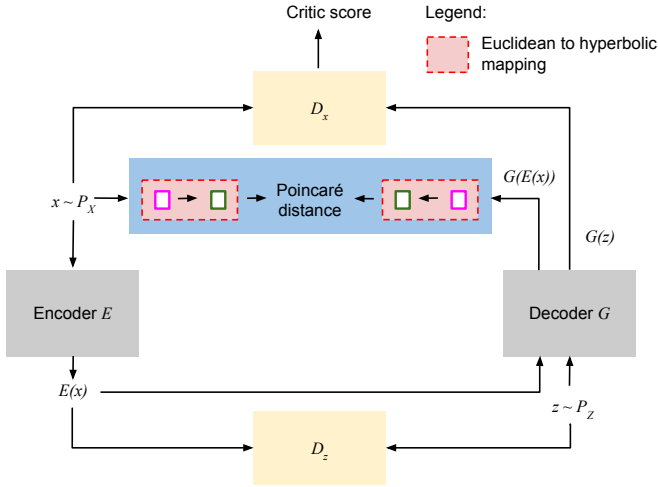


Fig. 2. Overall architecture of our proposed model HypAD. The model integrates hyperNNs [48] with an LSTM based encoder-decoder trained with two GAN-based discriminators, D_x and D_z . HypAD maps the input signal x and the output of the decoder ($G(E(x))$) to the Poincaré ball model of hyperbolic spaces, shown as dotted red edge box with red background, to get the corresponding hyperbolic embeddings. The two embeddings are then compared using Poincaré distance, as described in Section III-B1. Solid magenta and green boxes denote the input and output of the hyperbolic mapping, respectively.

split/concatenation operations, generalising the convolutional layer to hyperspace. [52], [53] propose hyperbolic graph neural networks, leveraging hyperNNs.

Thus formulated, hyperNNs have mainly been adopted to improve performance by leveraging hierarchies and uncertainty in zero-shot learning [54], re-identification [55], and action recognition [56]. Of particular interest, [20] has leveraged hyperNNs to model a hierarchy of actions from unlabeled videos. To the best of our knowledge, this is the first work to have applied hyperNNs for sequence modelling with the goal of anomaly detection.

III. METHOD

In this section, we first discuss best practises in anomaly detection (Section III-A); then we detail the proposed hyperbolic uncertainty and its use for detecting anomalies (Section III-B); finally we discuss the motivation for it (Section III-C).

A. Background

The current state-of-the-art in univariate anomaly detection is a reconstruction-based technique [9] which additionally leverages a GAN critic score. TadGAN encodes the input data x to a latent space and then decodes the encoded data. This encoding-decoding operation requires two mapping functions $E : X \rightarrow Z$ and $G : Z \rightarrow X$. The reconstruction operation can be given as $x \rightarrow E(x) \rightarrow G(E(x)) \rightarrow \tilde{x} \approx x$. TadGAN leverages adversarial learning to train the two mappings by using two adversarial critics D_x and D_z . The goal of D_x is to distinguish between the real and the generated time series, while D_z measures the performance of the mapping into latent space. The model is trained using the combination

of Wasserstein loss [57] and Cycle consistency loss [58]. TadGAN computes the reconstruction error $RE(x)$ between x and \tilde{x} using three types of reconstruction functions: **i.** Point-wise difference: considers the difference of values at every time stamp; **ii.** Area difference: is applied on signals of fixed lengths and measures the similarity between local regions; **iii.** Dynamic time warping: additionally handles time gaps between the two signals to calculate the reconstruction error.

To calculate the anomaly score, TadGAN first normalises the reconstruction error and critic scores by subtracting the mean and dividing by standard deviation. The normalised scores, $Z_{RE}(x)$ and $Z_{D_x}(x)$, are then combined using their product:

$$s_p(x) = Z_{RE}(x) \odot Z_{D_x}(x) \quad (1)$$

B. Hyperbolic uncertainty for Anomaly detection (HypAD)

We propose a novel model for anomaly detection in time series based on hyperbolic uncertainty. HypAD is a reconstruction-based model and minimises the reconstruction loss, given by a measure of the hyperbolic distance between the input signal and its reconstruction. In hyperbolic space, errors are exponentially larger when predictions are certain. Therefore, HypAD tends to predict either certain correct reconstructions or uncertain possibly mistaken reconstructions.

This leads, as we discuss in Sec. III-C, to a novel definition of detectable anomaly: i.e. the case of a large reconstruction error with high certainty.

1) *Hyperbolic Reconstruction Error*: The proposed HypAD is illustrated in Figure 2. It integrates the machinery of hyperbolic neural networks into the reconstruction-based architecture of TadGAN. In HypAD the input signal x is first passed through an encoder, then followed by a decoder sub-network. The output of the decoder $G(E(x))$ as well as the original signal x are mapped to the hyperspace, shown as the red edge box with red background.

An n -dimensional hyperspace is a Riemannian geometry with a constant negative sectional curvature. As in [20], [55], we adopt the Poincaré ball model of hyperspaces, given by the manifold $\mathbb{D}_n = \{x \in \mathbb{R}^n : \|x\| < 1\}$ endowed with the Riemannian metric $g^{\mathbb{D}}(x) = \lambda_x^2 g^E$, where $\lambda_x = \frac{2}{1-\|x\|^2}$ is the *conformal factor* and $g^E = I_n$ is the Euclidean metric tensor. For details, see [59], [60].

In order to map x and $G(E(x))$ to the Poincaré ball, we leverage an *exponential map* centered at $\mathbf{0}$ [20]. This is followed by a hyperbolic feed-forward layer [48] to estimate the corresponding hyperbolic embeddings h and \tilde{h} , shown as solid green boxes in Figure 2. Finally, the two hyperbolic embeddings are compared using the Poincaré distance, formulated as follows:

$$RE(x) = \cosh^{-1} \left(1 + 2 \frac{\|h - \tilde{h}\|^2}{(1 - \|h\|^2)(1 - \|\tilde{h}\|^2)} \right) \quad (2)$$

where $\|h\|^2$ and $\|\tilde{h}\|^2$ are the distances of the embeddings from the center of the Poincaré ball. Note that the same reconstruction error function $RE(x)$, is used at training as well as inference time.

2) *Hyperbolic Uncertainty* : A key property of the Poincaré ball is that the distance between two points grows exponentially as we move away from the origin. This means that an erroneous reconstruction towards the circumference of the disk is penalised exponentially more than an erroneous reconstruction close to the centre. This leads to the useful tendency of HypAD to either predict a matched reconstruction (\tilde{h} and h are close by) or an unmatched reconstruction towards the origin (\tilde{h} and h are far-away, $\|h\|^2$ and $\|\tilde{h}\|^2$ are small), in order to minimize Eq. (2).

Hence, the distance of the reconstruction to the origin provides a natural estimate of the model’s uncertainty, referred to as hyperbolic uncertainty, $U(X)$, thus formulated:

$$U(X) = 1 - \|\tilde{h}\|^2 \quad (3)$$

The smaller the distance from the origin, the more uncertain is the model.

3) *Combining Hyperbolic Uncertainty with Reconstruction Error and Critic Score*: Hyperbolic uncertainty $U(x)$ is integrated into the anomaly score as follows:

$$s_u(x) = Z_{RE}(x) \odot Z_{D_x}(x) \odot (1 - U(x)) \quad (4)$$

Equation 4 brings together the reconstruction error $Z_{RE}(x)$ (the larger the error, the more likely the anomaly) with the critic score $Z_{D_x}(x)$ (larger critic scores point to anomalies) and the model certainty: $1 - U(x)$.

The simple multiplication formulation of the certainty of the model reduces the scores of anomalies when HypAD is not confident of the reconstructions. While being simple, this outperforms the current state-of-the-art, as we show in Section IV.

C. Motivation for HypAD

HypAD takes motivation from a key idea: *a detectable anomaly is one where the model is certain, but it predicts wrongly*. In other words, if the model encounters a known pattern, which it knows how to reconstruct, then it will call it anomalous, if the reconstruction does not match the input signal.

The principled formulation of hyperbolic uncertainty is paramount towards this goal: HypAD predicts a reconstruction as uncertain if it is doubtful that it may be wrong.

Fig. 3 illustrates this key concept for all the datasets. The first, second and third rows correspond to the univariate, U-CASAS and SWaT datasets respectively. The bar plot depicts the average cosine distances between the input signals and their reconstructions, against specific intervals of uncertainty, along the x-axis. The higher the cosine distances, the more distinct the reconstruction is from the provided signals¹. Note that for the first two rows, the initial three plots (columns) correspond to the signals that report the best improvement in F1-score and the last plot corresponds to the signal with worst improvement. A single bar-plot is reported for SWaT because this consists of a single long-term signal.

Observe in the second row, how HypAD learns to correctly assign higher uncertainty to wronger estimates for the cases of Fall, Weakness, and Nocturia. For the last signal Slower-Walking, HypAD fails to learn a meaningful uncertainty and labels all reconstructions as certain. It is however notable that the representation is still interpretable and the case of failure discernible. Trends are similar for the cases of Univariate and SWaT datasets.

IV. RESULTS

We compare HypAD against the current best univariate anomaly detector TadGAN [9] on a benchmark of 11 time series, and extend the comparison to 2 multivariate sensor datasets: one comprising a water treatment plant and one comprising daily activities in elderly residences. First, we introduce the benchmarks (Sec. IV-A), then we compare against baselines and the state-of-the-art (Sec. IV-B), finally we conduct ablative studies on the importance of uncertainty for performance and the reduction of false alarms (Sec. IV-C).

A. Datasets, metrics and experimental setup

Table I summarizes the main characteristics of the datasets, which we coarsely divide into univariate, main test bed of our baseline TadGAN [9], and multivariate, to which we extend comparison. In the table, we report the sources of signals (NASA, Yahoo, NAB, CASAS and SWaT) and the datasets within each source (SMAP, MSL, A1 etc.), cf. detailed description later in the section.

In the table, the *number of signals* is the number of time series within the datasets. Note that univariate datasets are composed of multiple signals, while the multivariate only comprise single large time series. The *number of anomalies* counts the instances, within the time series, labelled as anomalous. These are further detailed as *point anomalies*, single anomalous values at a specific point in time, or *collective anomalies*, sets of contiguous times which are altogether anomalous. Yahoo is the sole dataset with point anomalies, and the only with *synthetic* sequences A2, A3, A4. We also report the *percentage of total* anomalous points and, following [9], for the univariate datasets, the *number of out-of-distribution* points, exceeding the means by more than 4σ .

a) *Univariate datasets*: NASA includes two spacecraft telemetry datasets² based on the Mars Science Laboratory (MSL) and the Soil Moisture Active Passive (SMAP) signals. The former consists of scientific and housekeeping engineering data taken from the Rover Environmental Monitoring Station aboard the Mars Science Laboratory. The latter includes measurements of soil moisture and freeze/thaw state from space for all non-liquid water surfaces globally within the top layer of the Earth.

We analyse *Yahoo* datasets based on real production traffic to Yahoo computing systems. Additionally, we consider three synthetic datasets coming from the same source³. The dataset tests the detection accuracy of various anomaly-types including outliers and change-points. The synthetic dataset consists

¹The Poincaré ball model is conformal to the Euclidean space and it preserves the same angles [51].

²<https://s3-us-west-2.amazonaws.com/telemanom/data.zip>.

³<https://webscope.sandbox.yahoo.com/catalog.php?datatype=s&did=70>

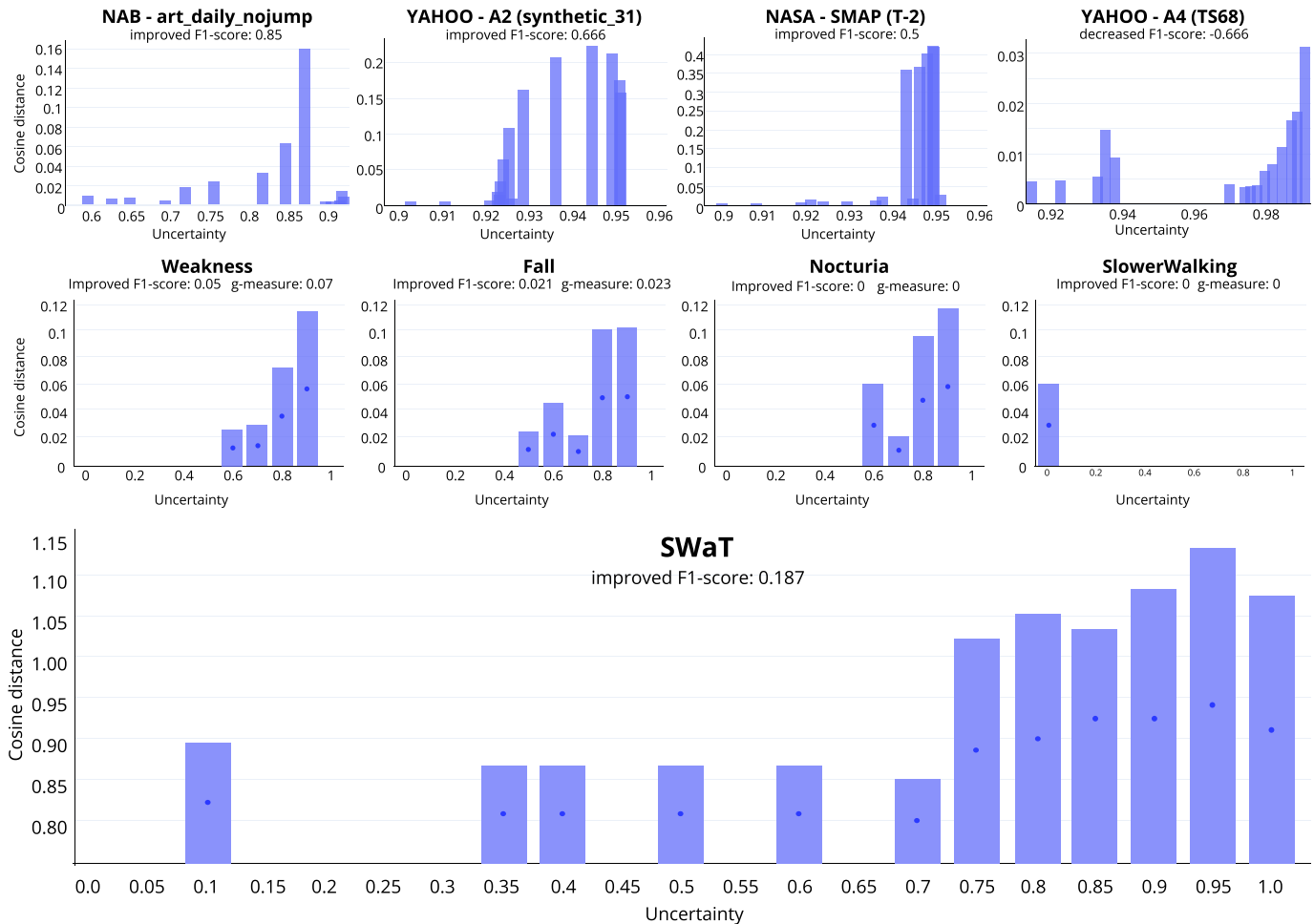


Fig. 3. Bar plot of the average cosine distance of all the datasets for specific intervals of uncertainty (see Sec. III-C). The first two rows contain three plots corresponding to the signals that report the best improvement in terms of F1-score (g-measure) and one plot (the last column) that corresponds to the signal with the worst improvement. Notice that even the signals with the worst improvement follow the same increasing trend. Because SWaT contains a single long-term signal, we report only its corresponding bar-plot.

of time-series with varying trend, noise and seasonality. The real dataset consists of time-series representing the metrics of various Yahoo services.

Numenta Anomaly Benchmark (NAB) is a well-established collection of univariate time-series from real-world application domains⁴. To be consistent with [9], we analyse Art, AdEx, AWS, Traf, and Tweets from the original collection.

b) Multivariate datasets: We consider for analysis the SWaT [23], [61] and CASAS [22], [62] datasets. *SWaT* is collected from a cyber-physical system testbed that is a scaled down replica of an industrial water treatment plant. The data was collected every second for a total of 11 days, where for the first few days the system was operated normally, while for the remaining days certain cyber-physical attacks were launched. Following [34], we sample sensor data every every 5 seconds.

CASAS is a collection of two weeks of sensor data from retirement homes. Each sensor reading has a label attached to it, according to the activity of elderly people recognised by human annotators. The 5 time series are a collection

of activities, grouped by the medical conditions established prior to the experimentation: Falling (F), More Time in Chair (MTC), Weakness (W), Slower Walking (SW), and Nocturia (N) for nightly time visits. Although sensor readings give fine-grained information, we are interested in creating daily patient profiles. Hence, we collapse them into a single engendered activity with a start and end time⁵ for each consecutive sensor signal. We then create a time matrix structure $\mathcal{M}^{|d|,1440}$ where $|d|$ is the number of days the patient is monitored and 1440 represent the total number of minutes in a day. $\mathcal{M}[i,j]$ represents the label performed in minute j of day i . Lastly, we densify each value $\mathcal{M}[i,j]$ with contextual and duration information corresponding to the label therein.

Finally, we create train and test splits of this data, caring to safeguard sequentiality of observations, and gathering the few anomalies into the test set for evaluation only. For this reason we name this Unsupervised-CASAS, dubbed U-CASAS, differing from the original CASAS [22], [62] since the latter interleaves anomalous sensor readings with normal

⁴We invite the reader to consult <https://github.com/numenta/NAB/tree/master/data> for the entire directory of datasets.

⁵The start time corresponds to the first sensor reading for that activity, whereas the end time is the last reading.

TABLE I

OVERVIEW OF SELECTED UNIVARIATE AND MULTIVARIATE DATASETS AND THEIR CHARACTERISTICS, GROUPED BY THE SOURCES OF SIGNALS (NASA, YAHOO, NAB, CASAS AND SWAT). SEE SEC. IV-A FOR DETAILS.

	Univariate										Multivariate						
	NASA		Yahoo				NAB				CASAS			SWaT			
	SMAP	MSL	A1	A2	A3	A4	Art	AdEx	AWS	Traf	Tweets	F	MTC	W	SW	N	
Num. of signals	53	27	67	100	100	100	6	5	17	7	10	1	1	1	1	1	1
Num. of anomalies	67	36	178	200	939	835	6	11	30	14	33	2	2	4	2	2	33
Point anomalies	0	0	68	33	935	833	0	0	0	0	0	0	0	0	0	0	0
Collective anomalies	67	36	110	167	4	2	6	11	30	14	33	2	2	4	2	2	33
Num. of anomaly points	54,696	7,766	1,699	466	943	837	2,418	795	6,312	1,560	15,651	99	239	1,248	276	1,060	10786
Percentage of total	9.7%	5.8%	1.8%	0.3%	0.6%	0.5%	10%	9.9%	9.3%	9.8%	9.8%	0.7%	1.7%	8%	2.4%	6.3%	10.05%
Num. out of distribution	18,126	642	861	153	21	49	123	15	210	86	520	-	-	-	-	-	-
Num. of instances	~563k	~132k	~95k	~142k	168k	168k	~24k	~8k	~68k	~16k	~159k	~54k	~276k	~39k	~39k	~39k	~189k
Synthetic?	No	No	No	Yes	Yes	Yes	Yes	No	No	No	No	No	No	No	No	No	No

TABLE II

RESULTS ON THE UNIVARIATE DATASETS FROM NASA, YAHOO AND NAB, MEASURED IN TERMS OF F1-SCORE. THE ENTRY TADGAN [9] IS REPORTED FROM THE PAPER. TADGAN* REFERS TO ITS REPRODUCED RESULT WITH THE PYTORCH VERSION (SEE SECS. IV-A, IV-B). MEAN μ AND STANDARD DEVIATION σ ARE COMPUTED ACROSS ALL DATASETS.

	NASA		YAHOO				NAB						F1 ($\mu \pm \sigma$)
	MSL	SMAP	A1	A2	A3	A4	Art	AdEx	AWS	Traf	Tweets		
TadGAN [9]	0.623	0.680	0.668	0.820	0.631	0.497	0.667	0.667	0.610	0.455	0.605	0.629 \pm 0.123	
AE	0.199	0.270	0.283	0.008	0.100	0.073	0.283	0.100	0.239	0.088	0.296	0.176 \pm 0.099	
LstmAE	0.317	0.318	0.310	0.023	0.097	0.089	0.261	0.130	0.223	0.136	0.299	0.200 \pm 0.103	
ConvAE	0.300	0.292	0.301	0.000	0.103	0.073	0.289	0.129	0.254	0.082	0.301	0.212 \pm 0.096	
TadGAN*	0.500	0.580	0.620	0.865	0.750	0.576	0.420	0.550	0.670	0.480	0.590	0.600 \pm 0.115	
HypAD (proposed)	0.565	0.643	0.610	0.670	0.670	0.470	0.777	0.663	0.630	0.570	0.670	0.631 \pm 0.075	

instances, thus breaking the sequentiality of anomalies. For each anomalous day encountered in the test set, we pad two days prior to it and two after. If the padding overlaps with another anomalous day, then we concatenate⁶ them and perform the padding procedure again. We delete the days assigned to the test set from the overall dataset and assign the rest as training. Moreover, because we employ a time-related strategy, we create time windows of 30 actions to detect anomalies.

c) Metrics: Being all the enlisted datasets highly unbalanced, accuracy is misleading. Therefore, as done in [20], we use the F1 score to account for this challenge. Notice that we do not use the cumulative F1 score as proposed in [63] to evaluate the performances because not all datasets contain anomalous events; rather they contain anomalous data points. Based on [64], for the univariate and the CASAS datasets, we penalize high false positive rates and encourage the detection of true positives in a timely fashion. Since anomalies are rare events and come in collective sequences in real-world applications, we proceed as follows:

- 1) We record a true positive (TP) if any predicted window overlaps a true anomalous window.
- 2) We record a false negative (FN) if a true anomalous window does not overlap any predicted window.
- 3) We record a false positive (FP) if a predicted window does not overlap any true anomalous region.

For U-CASAS, we also measure the g-measure which is the geometric mean of the product of recall (R) and precision (P), being a robust metric when classes are imbalanced [62].

d) Baselines: We include the following strategies as our baselines in this paper:

- *AE* [65] - We use a six-layer fully-connected autoencoder.
- *ConvAE* [66] - We have three layers of convolutional encoding interleaved with max pooling. The decoder has a specular composition as the encoder where the deconvolution is aided by two-dimensional up-sampling layers.
- *LstmAE* [67] - We use a deep stacked LSTM autoencoder with four layers. The first LSTM hidden and output vectors get passed to the second LSTM layer. The latent representation of the encoder gets then reconstructed in reverse order from the decoder.
- *TadGAN** [9] - We use a one-layer bidirectional LSTM for the generator E , and a two-layer bidirectional LSTM for G . For the critic D_z we use a fully connected layer, and two dense layers for D_x .

Implementation details. For the first three baselines, we set the number of epochs to 30, the batch size to 32, and the learning rate to 10^{-3} . For TadGAN*, we set the epochs to 30, the batch size to 64, the learning rate to 5×10^{-4} , and the iteration for the critic to 5. We use Adam as the optimisation function to train all the baselines.

For our proposed method HypAD, we took inspiration from an online available PyTorch implementation⁷. We leave the architecture of TadGAN unvaried, but we incorporate the hyperbolic transformation⁸ as in [20]. The hyperparameters are the same in the original paper, but we use the Riemannian Adam⁹ as optimisation function.

B. Comparison to the state of the art

HypAD defines a new state-of-the-art performance for univariate anomaly detection by having the highest average

⁶The concatenation procedure merges common sequences. If the sequence contains more than one anomalous day within the two-day padding window, the padded sequence gets collapsed into a single one.

⁷<https://github.com/aronppsg/TadGAN>

⁸<https://github.com/cvlab-columbia/hyperfuture>

⁹<https://github.com/geoopt/geoopt>

TABLE III

RESULTS FOR THE U-CASAS MULTIVARIATE DATASETS, MEASURED IN TERMS OF F1-SCORE AND G-MEASURE. TADGAN* REFERS ITS PYTORCH VERSION (SEE SECS. IV-A, IV-B). THE DATASETS FOR THE SPECIFIC MEDICAL CONDITIONS AS ABBREVIATED AS SUCH: FALLING (F), MORE TIME IN CHAIR (MTC), WEAKNESS (W), SLOWER WALKING (SW), AND NOCTURIA (N).

	F		W		N		SW		MTC		g-measure ($\mu \pm \sigma$)	F1 ($\mu \pm \sigma$)
	g-measure	F1	g-measure	F1	g-measure	F1	g-measure	F1	g-measure	F1		
LstmAE	0.085	0.014	0.182	0.108	0.000	0.000	0.158	0.049	0.133	0.035	0.112 \pm 0.064	0.041 \pm 0.037
AE	0.139	0.127	0.033	0.027	0.116	0.103	0.000	0.000	0.158	0.049	0.089 \pm 0.062	0.061 \pm 0.047
ConvAE	0.086	0.014	0.284	0.150	0.251	0.119	0.158	0.048	0.134	0.035	0.183 \pm 0.074	0.073 \pm 0.052
TadGAN*	0.222	0.267	0.570	0.555	0.000	0.000	0.630	0.570	0.267	0.222	0.338 \pm 0.233	0.323 \pm 0.216
HypAD (proposed)	0.447	0.333	0.660	0.610	0.447	0.333	0.470	0.364	0.577	0.5	0.520 \pm 0.095	0.428 \pm 0.123

TABLE IV

RESULTS ON THE SWAT DATASET, IN TERMS OF F1-SCORE, INCLUDING THE CORRESPONDING PREDICTION AND RECALL. TADGAN* REFERS TO THE PYTORCH VERSION.

Model	Precision	Recall	F1
EncDec-AD [42] [ICML-WorkShop16]	0.945	0.620	0.748
DAGMM [68][ICLR18]	0.946	0.747	0.835
OmniAnomaly [35] [KDD19]	0.979	0.757	0.854
USAD [69] [KDD20]	0.987	0.740	0.846
TadGAN* [BigData20]	0.937	0.587	0.722
NSIBF [34] [KDD21]	0.982	0.863	0.919
HypAD (Ours)	0.996	0.605	0.753

F1-scores of 0.631. In Table II, HypAD outperforms the current best technique (TadGAN*, 0.600) by 5.17%, as well as all baselines by a large margin. Note that we also report the original paper [9] performance of TadGAN in the first row (0.629), which we could not reproduce with the available PyTorch code (cf. Sec. IV-A). In the Table, the column *F1* reports mean μ and standard deviation σ over all datasets. Looking at $\sigma = 0.075$, HypAD also appears as the most consistent performer. Considering the F1-score, the largest performance gain of HypAD Vs TadGAN are on NAB and NASA datasets, while it is outperformed more largely on the A2, A3 and A4 Yahoo datasets, the sole synthetic univariate ones.

In Table III, we extend the evaluation of HypAD to the multivariate U-CASAS dataset. We cannot include Isudra [62] because the underlying architecture uses a small amount of labels to conduct the selection of parameters for the execution. Additionally, Isudra is trained in a supervised fashion differing from all the other methods reported here. For completeness, we also report the g-measure [62] and its average across all datasets. As shown in the table, HypAD surpasses TadGAN* by 32.51% in terms of average F1-score (0.428 Vs. 0.323).

Finally, in Table IV, we also extend comparison to the multivariate SWaT dataset. Here, following previous work [34], we also report the precision and recall in addition to the F1-score. HypAD outperforms the baseline TadGAN* (0.753 Vs. 0.722) but both techniques are behind the current state-of-the-art on multivariate anomaly detection, NSIBF [34]. Observe however that HypAD achieves its highest F1-performance at the highest precision (0.996) among all other methods. This confirms that HypAD really detects anomalies which it is certain about, i.e. when it *understands* the time series and it is certain about what to expect, but cannot reconstruct the input signal due to an anomaly.

TABLE V

ABLATIVE EVALUATION ON THE IMPORTANCE OF THE HYPERBOLIC MAPPING AND THE INTEGRATION OF UNCERTAINTY. AVERAGE F1-SCORES ARE REPORTED FOR UNIVARIATE, U-CASAS AND SWAT DATASETS.

	Univariate	U-CASAS	SWaT
Euclidean (TadGAN)	0.600	0.323	0.722
Hyperbolic	0.604	0.397	0.566
Hyperbolic + Uncertainty (HypAD)	0.631	0.428	0.753

C. Ablation Studies

In Table V, we analyze the importance of the hyperbolic embedding and the use of uncertainty for anomaly detection on the univariate datasets, as well as the multivariate U-CASAS and SWaT. The first row shows the performance of the model in Euclidean space (average F1-score across datasets). This corresponds to TadGAN* in Table II, III and IV. In the second row, we report performance for the hyperbolic TadGAN*, without including uncertainty (cf. Sec. III-B1). This improves marginally over the univariate (0.604 Vs. 0.600) and more importantly over the U-CASAS datasets (0.397 Vs. 0.323), but it decreases performance in SWaT (0.566 Vs. 0.722), which we further analyze in the following subsection.

The complete proposed HypAD model, in the third row, improves consistently on both ablative variants. HypAD yields 0.631 on the univariate datasets, 0.428 on U-CASAS, and 0.753 on SWaT. Improvements *wrt* not using uncertainty are large, respectively 4.5%, 7.8% and 33%. We therefore conclude that **uncertainty is fundamental for ameliorating anomaly detection.**

Qualitative Ablation on SWaT: In Figure 4, we demonstrate qualitative ablation on the SWaT dataset, which consists of a single long signal. The three plots correspond to the three ablative variants of Table V. In all plots, the blue and green points represent the predicted anomaly scores and the ground-truth anomalies, respectively. The red line denotes the anomaly detection threshold i.e. blue points above the red line are the predicted anomalies. False positives are blue points above the red line threshold outside the green (ground-truth) anomalous regions.

As it shows in the figure, the Euclidean model (first plot) yields many false positives; the hyperbolic model w/o uncertainty (second plot) reduces the number of false positives substantially, but it also misses anomalies, esp. in the middle signal part. This explains the drop in the F-1 score for the SWaT dataset (cf. Table V). Integrating hyperbolic uncertainty (proposed HypAD, third plot) recovers detection of these

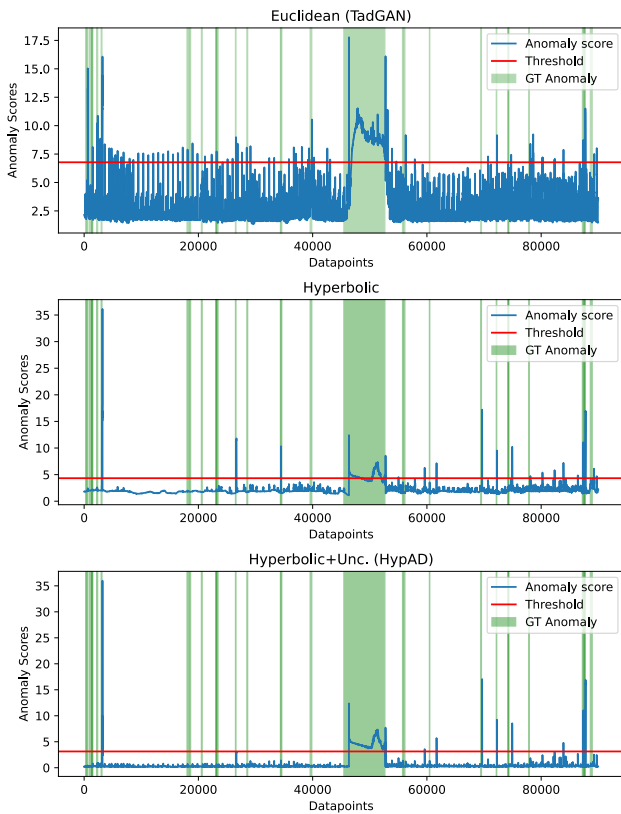


Fig. 4. Qualitative Ablation on SWaT: The anomaly scores (blue points) that lie above the anomaly detection threshold (red line) but do not coincide with the ground-truth (green points) are false positives. The Euclidean model in plot 1 has many false positives. The corresponding hyperbolic model in plot 2 is more precise but loses some true positives, especially in the middle region. The integration of uncertainty helps to recover these points, increasing the true positives and overall F-1 score (See Sec IV-C).

anomalies, it increases true positives but maintains the number of false positives low, thus yielding the best F1 score of 0.753.

V. CONCLUSIONS

We have proposed a novel model for anomaly detection based on hyperbolic uncertainty, HypAD. The proposed hyperbolic uncertainty allows HypAD to self-adjusts its output, encouraging the model to either predict a correct reconstruction or a less certain wrong reconstruction. This benefits anomaly detection in two ways: it provides better reconstructions of the signal (the deviation from those being anomalous) and it yields a measure of certainty. This is a novel viewpoint on anomaly detection: detectable anomaly instances are those which are certain but wrongly predicted.

REFERENCES

- [1] H. Fan, O. R. Zaïane, A. Foss, and J. Wu, "A nonparametric outlier detection for effectively discovering top-n outliers from engineering data," in *Pacific-Asia conference on knowledge discovery and data mining*. Springer, 2006, pp. 557–566.
- [2] A. Ghoting, S. Parthasarathy, and M. E. Otey, "Fast mining of distance-based outliers in high-dimensional datasets," *Data Mining and Knowledge Discovery*, vol. 16, no. 3, pp. 349–364, 2008.
- [3] M. M. Breunig, H.-P. Kriegel, R. T. Ng, and J. Sander, "Lof: identifying density-based local outliers," in *ACM sigmod record*, vol. 29. ACM, 2000, pp. 93–104.
- [4] S. Papadimitriou, H. Kitagawa, P. B. Gibbons, and C. Faloutsos, "LocI: Fast outlier detection using the local correlation integral," in *Proceedings 19th International Conference on Data Engineering (Cat. No. 03CH37405)*. IEEE, 2003, pp. 315–326.
- [5] F. Keller, E. Muller, and K. Bohm, "Hics: High contrast subspaces for density-based outlier ranking," in *2012 IEEE 28th international conference on data engineering*. IEEE, 2012, pp. 1037–1048.
- [6] A. Lazarevic and V. Kumar, "Feature bagging for outlier detection," in *Proceedings of the eleventh ACM SIGKDD international conference on Knowledge discovery in data mining*. ACM, 2005, pp. 157–166.
- [7] J. Chen, S. Sathe, C. Aggarwal, and D. Turaga, "Outlier detection with autoencoder ensembles," in *Proceedings of the 2017 SIAM International Conference on Data Mining*. SIAM, 2017, pp. 90–98.
- [8] H. Sarvari, C. Domeniconi, B. Prencakj, and G. Stilo, "Unsupervised boosting-based autoencoder ensembles for outlier detection," in *PAKDD (1)*. Springer, 2021, pp. 91–103.
- [9] A. Geiger, D. Liu, S. Alneghimeh, A. Cuesta-Infante, and K. Veeramachaneni, "Tadgan: Time series anomaly detection using generative adversarial networks," in *2020 IEEE International Conference on Big Data (Big Data)*. IEEE, 2020, pp. 33–43.
- [10] B. Lakshminarayanan, A. Pritzel, and C. Blundell, "Simple and scalable predictive uncertainty estimation using deep ensembles," *arXiv preprint arXiv:1612.01474*, 2016.
- [11] A. Kendall and Y. Gal, "What uncertainties do we need in bayesian deep learning for computer vision?" *arXiv preprint arXiv:1703.04977*, 2017.
- [12] Y. Gal and Z. Ghahramani, "Dropout as a bayesian approximation: Representing model uncertainty in deep learning," in *international conference on machine learning*. PMLR, 2016, pp. 1050–1059.
- [13] B. Jiang, R. Luo, J. Mao, T. Xiao, and Y. Jiang, "Acquisition of localization confidence for accurate object detection," in *Proceedings of the European conference on computer vision (ECCV)*, 2018, pp. 784–799.
- [14] F. Kuppens, J. Kronenberger, A. Shantia, and A. Haselhoff, "Multivariate confidence calibration for object detection," in *Proceedings of the IEEE/CVF Conference on Computer Vision and Pattern Recognition Workshops*, 2020, pp. 326–327.
- [15] Z. Li and D. Hoiem, "Improving confidence estimates for unfamiliar examples," in *2020 IEEE/CVF Conference on Computer Vision and Pattern Recognition (CVPR)*, 2020, pp. 2683–2692.
- [16] L. Neumann, A. Zisserman, and A. Vedaldi, "Relaxed softmax: Efficient confidence auto-calibration for safe pedestrian detection," 2018.
- [17] A. Vakhitov, L. Ferraz, A. Agudo, and F. Moreno-Noguer, "Uncertainty-aware camera pose estimation from points and lines," in *Proceedings of the IEEE/CVF Conference on Computer Vision and Pattern Recognition*, 2021, pp. 4659–4668.
- [18] A. Hu, Z. Murez, N. Mohan, S. Dudas, J. Hawke, V. Badrinarayanan, R. Cipolla, and A. Kendall, "FIERY: Future instance segmentation in bird's-eye view from surround monocular cameras," in *Proceedings of the International Conference on Computer Vision (ICCV)*, 2021.
- [19] E. Sanginetto, M. Nabi, D. Culibrk, and N. Sebe, "Self paced deep learning for weakly supervised object detection," *IEEE Transactions on Pattern Analysis and Machine Intelligence*, vol. 41, no. 3, pp. 712–725, 2019.
- [20] D. Suris, R. Liu, and C. Vondrick, "Learning the predictability of the future," in *Proceedings of the IEEE/CVF Conference on Computer Vision and Pattern Recognition*, 2021, pp. 12 607–12 617.
- [21] A. Lavin and S. Ahmad, "Evaluating real-time anomaly detection algorithms—the numenta anomaly benchmark," in *2015 IEEE 14th International Conference on Machine Learning and Applications (ICMLA)*. IEEE, 2015, pp. 38–44.
- [22] D. J. Cook, A. S. Crandall, B. L. Thomas, and N. C. Krishnan, "Casas: A smart home in a box," *Computer*, vol. 46, no. 7, pp. 62–69, 2012.
- [23] A. P. Mathur and N. O. Tippenhauer, "Swat: a water treatment testbed for research and training on ics security," *2016 International Workshop on Cyber-physical Systems for Smart Water Networks (CySWater)*, pp. 31–36, 2016.
- [24] T. G. Dietterich, "Ensemble methods in machine learning," in *International workshop on multiple classifier systems*. Springer, 2000, pp. 1–15.
- [25] I. Goodfellow, J. Pouget-Abadie, M. Mirza, B. Xu, D. Warde-Farley, S. Ozair, A. Courville, and Y. Bengio, "Generative adversarial nets," *Advances in neural information processing systems*, vol. 27, 2014.

- [26] Y. Du and I. Mordatch, "Implicit generation and modeling with energy based models," *Advances in Neural Information Processing Systems*, vol. 32, pp. 3608–3618, 2019.
- [27] R. Salakhutdinov and G. Hinton, "Deep boltzmann machines," in *Artificial intelligence and statistics*. PMLR, 2009, pp. 448–455.
- [28] J. Xie, Y. Lu, S.-C. Zhu, and Y. Wu, "A theory of generative convnet," in *International Conference on Machine Learning*. PMLR, 2016, pp. 2635–2644.
- [29] J. Zhang, Y. Dai, M. Xiang, D.-P. Fan, P. Moghadam, M. He, C. Walder, K. Zhang, M. Harandi, and N. Barnes, "Dense uncertainty estimation," *arXiv preprint arXiv:2110.06427*, 2021.
- [30] J. Xie, Y. Lu, R. Gao, S.-C. Zhu, and Y. N. Wu, "Cooperative training of descriptor and generator networks," *IEEE transactions on pattern analysis and machine intelligence*, vol. 42, no. 1, pp. 27–45, 2018.
- [31] E. M. Knorr and R. T. Ng, "Algorithms for mining distance-based outliers in large datasets," in *Vldb*. Morgan Kaufmann, 1998, pp. 392–403. [Online]. Available: <http://dblp.uni-trier.de/db/conf/vldb/vldb98.html#KnorrN98>
- [32] F. Angiulli and C. Pizzuti, "Fast outlier detection in high dimensional spaces," in *European Conference on Principles of Data Mining and Knowledge Discovery*. Springer, 2002, pp. 15–27.
- [33] Z. He, X. Xu, and S. Deng, "Discovering cluster-based local outliers," *Pattern Recognit. Lett.*, vol. 24, pp. 1641–1650, 2003.
- [34] C. Feng and P. Tian, "Time series anomaly detection for cyber-physical systems via neural system identification and bayesian filtering," in *The 27th ACM SIGKDD Conference on Knowledge Discovery and Data Mining*. ACM, 2021, pp. 2858–2867.
- [35] Y. Su, Y. Zhao, C. Niu, R. Liu, W. Sun, and D. Pei, "Robust anomaly detection for multivariate time series through stochastic recurrent neural network," in *Proceedings of the 25th ACM SIGKDD International Conference on Knowledge Discovery & Data Mining*. ACM, 2019, p. 2828–2837.
- [36] Z. Wang, Z. Chen, J. Ni, H. Liu, H. Chen, and J. Tang, "Multi-scale one-class recurrent neural networks for discrete event sequence anomaly detection," in *The 27th ACM SIGKDD Conference on Knowledge Discovery and Data Mining*. ACM, 2021, pp. 3726–3734.
- [37] Y. Su, Y. Zhao, C. Niu, R. Liu, W. Sun, and D. Pei, "Robust anomaly detection for multivariate time series through stochastic recurrent neural network," in *Proceedings of the 25th ACM SIGKDD international conference on knowledge discovery & data mining*, 2019, pp. 2828–2837.
- [38] S.-E. Benkabou, K. Benabdeslem, V. Kraus, K. Bourhis, and B. Canitia, "Local anomaly detection for multivariate time series by temporal dependency based on poisson model," *IEEE Transactions on Neural Networks and Learning Systems*, 2021.
- [39] S. Ahmad, A. Lavin, S. Purdy, and Z. Agha, "Unsupervised real-time anomaly detection for streaming data," *Neurocomputing*, vol. 262, pp. 06–17, 2017.
- [40] K. Hundman, V. Constantinou, C. Laporte, I. Colwell, and T. Söderström, "Detecting spacecraft anomalies using lstms and non-parametric dynamic thresholding," in *KDD*. ACM, 2018, pp. 387–395.
- [41] J. An and S. Cho, "Variational autoencoder based anomaly detection using reconstruction probability," in *Special Lecture on IE*, vol. 2, pp. 2015.
- [42] P. Malhotra, A. Ramakrishnan, G. Anand, L. Vig, P. Agarwal, and G. M. Shroff, "Lstm-based encoder-decoder for multi-sensor anomaly detection," *ArXiv*, vol. abs/1607.00148, 2016.
- [43] A. Abdulaal, Z. Liu, and T. Lancewicki, "Practical approach to asynchronous multivariate time series anomaly detection and localization," in *Proceedings of the 27th ACM SIGKDD Conference on Knowledge Discovery & Data Mining*. ACM, 2021, p. 2485–2494.
- [44] Z. Li, Y. Zhao, J. Han, Y. Su, R. Jiao, X. Wen, and D. Pei, "Multivariate time series anomaly detection and interpretation using hierarchical inter-metric and temporal embedding," in *Proceedings of the 27th ACM SIGKDD Conference on Knowledge Discovery & Data Mining*, 2021, pp. 3220–3230.
- [45] L. Li, J. Yan, H. Wang, and Y. Jin, "Anomaly detection of time series with smoothness-inducing sequential variational auto-encoder," *IEEE transactions on neural networks and learning systems*, vol. 32, no. 3, pp. 1177–1191, 2020.
- [46] D. Li, D. Chen, L. Shi, B. Jin, J. Goh, and S.-K. Ng, "Mad-gan: Multivariate anomaly detection for time series data with generative adversarial networks," in *ICANN*, 2019.
- [47] B. Zhou, S. Liu, B. Hooi, X. Cheng, and J. Ye, "Beatgan: Anomalous rhythm detection using adversarially generated time series," in *Proceedings of the Twenty-Eighth International Joint Conference on Artificial Intelligence, IJCAI-19*. International Joint Conferences on Artificial Intelligence Organization, 7 2019, pp. 4433–4439. [Online]. Available: <https://doi.org/10.24963/ijcai.2019/616>
- [48] O. Ganea, G. Becigneul, and T. Hofmann, "Hyperbolic neural networks," in *Advances in Neural Information Processing Systems*, S. Bengio, H. Wallach, H. Larochelle, K. Grauman, N. Cesa-Bianchi, and R. Garnett, Eds., vol. 31. Curran Associates, Inc., 2018. [Online]. Available: <https://proceedings.neurips.cc/paper/2018/file/dbab2adc8f9d078009ee3fa810bea142-Paper.pdf>
- [49] C. Gulcehre, M. Denil, M. Malinowski, A. Razavi, R. Pascanu, K. M. Hermann, P. Battaglia, V. Bapst, D. Raposo, A. Santoro, and N. de Freitas, "Hyperbolic attention networks," in *International Conference on Learning Representations*, 2019. [Online]. Available: <https://openreview.net/forum?id=rJxHsjRqFQ>
- [50] A. Lou, I. Katsman, Q. Jiang, S. J. Belongie, S.-N. Lim, and C. D. Sa, "Differentiating through the fréchet mean," *ArXiv*, vol. abs/2003.00335, 2020.
- [51] R. Shimizu, Y. Mukuta, and T. Harada, "Hyperbolic neural networks++," in *International Conference on Learning Representations*, 2021. [Online]. Available: <https://openreview.net/forum?id=Ec85b0tUwba>
- [52] Q. Liu, M. Nickel, and D. Kiela, "Hyperbolic graph neural networks," in *Advances in Neural Information Processing Systems*, H. Wallach, H. Larochelle, A. Beygelzimer, F. d'Alché-Buc, E. Fox, and R. Garnett, Eds., vol. 32. Curran Associates, Inc., 2019. [Online]. Available: <https://proceedings.neurips.cc/paper/2019/file/103303dd56a731e377d01f6a37badae3-Paper.pdf>
- [53] I. Chami, Z. Ying, C. Ré, and J. Leskovec, "Hyperbolic graph convolutional neural networks," *Advances in neural information processing systems*, vol. 32, pp. 4868–4879, 2019.
- [54] S. Liu, J. Chen, L. Pan, C.-W. Ngo, T.-S. Chua, and Y.-G. Jiang, "Hyperbolic visual embedding learning for zero-shot recognition," in *IEEE/CVF Conference on Computer Vision and Pattern Recognition (CVPR)*, June 2020.
- [55] V. Khruikov, L. Mirvakhabova, E. Ustinova, I. Oseledets, and V. Lempitsky, "Hyperbolic image embeddings," in *IEEE/CVF Conference on Computer Vision and Pattern Recognition (CVPR)*, June 2020.
- [56] T. Long, P. Mettes, H. T. Shen, and C. G. M. Snoek, "Searching for actions on the hyperbole," in *2020 IEEE/CVF Conference on Computer Vision and Pattern Recognition (CVPR)*, 2020, pp. 1138–1147.
- [57] M. Arjovsky, S. Chintala, and L. Bottou, "Wasserstein generative adversarial networks," in *Proceedings of the 34th International Conference on Machine Learning*, ser. Proceedings of Machine Learning Research, D. Precup and Y. W. Teh, Eds., vol. 70. PMLR, 06–11 Aug 2017, pp. 214–223.
- [58] J.-Y. Zhu, T. Park, P. Isola, and A. A. Efros, "Unpaired image-to-image translation using cycle-consistent adversarial networks," in *2017 IEEE International Conference on Computer Vision (ICCV)*, 2017, pp. 2242–2251.
- [59] J. M. Lee, *Riemannian Manifolds: An Introduction to Curvature*. Springer Science & Business Media, 2006, vol. 176.
- [60] —, *Smooth manifolds. In Introduction to Smooth Manifolds*. Springer, 2013.
- [61] J. Goh, S. Adepu, K. N. Junejo, and A. Mathur, "A dataset to support research in the design of secure water treatment systems," in *Critical Information Infrastructures Security*. Springer International Publishing, 2017, pp. 88–99.
- [62] J. Dahmen and D. J. Cook, "Indirectly supervised anomaly detection of clinically meaningful health events from smart home data," *ACM Transactions on Intelligent Systems and Technology (TIST)*, vol. 12, no. 2, pp. 1–18, 2021.
- [63] A. Garg, W. Zhang, J. Samaran, R. Savitha, and C.-S. Foo, "An evaluation of anomaly detection and diagnosis in multivariate time series," *IEEE Transactions on Neural Networks and Learning Systems*, vol. 33, no. 6, pp. 2508–2517, 2021.
- [64] K. Hundman, V. Constantinou, C. Laporte, I. Colwell, and T. Soderstrom, "Detecting spacecraft anomalies using lstms and nonparametric dynamic thresholding," in *Proceedings of the 24th ACM SIGKDD international conference on knowledge discovery & data mining*, 2018, pp. 387–395.
- [65] P. Baldi, "Autoencoders, unsupervised learning, and deep architectures," in *Proceedings of ICML workshop on unsupervised and transfer learning*. JMLR Workshop and Conference Proceedings, 2012, pp. 37–49.
- [66] M. Maggipinto, C. Masiero, A. Beghi, and G. A. Susto, "A convolutional autoencoder approach for feature extraction in virtual metrology," *Procedia Manufacturing*, vol. 17, pp. 126–133, 2018.
- [67] A. Sagheer and M. Kotb, "Unsupervised pre-training of a deep lstm-based stacked autoencoder for multivariate time series forecasting problems," *Scientific reports*, vol. 9, no. 1, pp. 1–16, 2019.

- [68] B. Zong, Q. Song, M. R. Min, W. Cheng, C. Lumezanu, D. Cho, and H. Chen, "Deep autoencoding gaussian mixture model for unsupervised anomaly detection," in *International conference on learning representations*, 2018.
- [69] J. Audibert, P. Michiardi, F. Guyard, S. Marti, and M. A. Zuluaga, "Usad: Unsupervised anomaly detection on multivariate time series," in *Proceedings of the 26th ACM SIGKDD International Conference on Knowledge Discovery & Data Mining*. ACM, 2020, p. 3395–3404.

Alessandro Flaborea is a PhD student at Sapienza University of Rome. He received his degree in Computer Science from the University of Udine, Italy, and his master's degree in Data Science from the Sapienza University of Rome.

His research interests include few-shot learning, person search, time series and video anomaly detection, pose estimation.

Bardh Prenkaj completed his PhD in February 2022 at Sapienza University of Rome in time-series analysis and anomaly detection. From 2019 onward, he has been a Researcher in the IIM research group of Computer Science Department at Sapienza University of Rome.

His research interests are across three areas: anomaly detection, educational data mining, and time series predictions. More in detail, his studies include investigations on student dropout prediction, anomaly detection on symbolic behavioural patterns, and drift anomaly detection.

Bharti Munjal is a PhD student at the Technical University of Munich (TUM), Germany. She received her engineering degree from the National Institute of Technology Kurukshetra India and her masters degree from TUM.

Her research interests include object detection, person search, person re-identification, few-shot learning and anomaly detection.

Marco Aurelio Sterpa is a MSc student at Sapienza University of Rome. He received his bachelor degree in Computer Science from Sapienza University of Rome and he is currently a second year master degree student in Data Science.

His research interests include time series and video anomaly detection.

Dario Aragona is a PhD student at Sapienza University of Rome, where he completed his master degree in Computer Science. His PhD belongs to the Italian National PhD Program in Artificial Intelligence, and his research topics include time series analysis and forecasting as well as anomaly detection.

Luca Podo is a PhD student in Computer Science at the University of Sapienza, with particular attention to Machine Learning, applied to data analysis. He got a master's degree in "Machine Learning Applied to the Visual Analytics of health conditions in older people" at the University of Sapienza.

His subjects of study are Artificial Intelligence and Data and Visual Analytics.

Fabio Galasso heads the Perception and Intelligence Lab (PINLab) at the Dept. of Computer Science, Sapienza University of Rome (Italy).

His research interests include distributed and multi-agent intelligent systems, perception (detection, recognition, re-identification, forecasting) and general intelligence (reasoning, meta-learning, domain adaptation), within sustainable (low-power-consumption and constrained-computational-resource sensors and devices) and interpretable (interpretable and verifiable AI) frameworks.